Quantitative Studies on the Melittin-Induced Leakage Mechanism of Lipid Vesicles†

Sybille Rex‡ and Gerhard Schwarz*

Department of Biophysical Chemistry, Biocenter of the University of Basel, Basel, Switzerland

Received April 30, 1997; Revised Manuscript Received August 29, 1997

ABSTRACT: We have investigated, both experimentally and theoretically, the efflux of carboxyfluorescein (a self-quenching fluorescent dye) from vesicles of different sizes and lipid species (POPC, DOPC) after having added the bee venom peptide melittin. This comprises quantitative analyses regarding the extent of lipid-associated peptide, the mode as well as the temporal progress of dye release and the possible leakage mechanism. Our results indicate a graded efflux characterized by a single-pore retention factor reflecting the formation of pores whose lifetimes are rather small (millisecond range). The observed fluorescence signal arising from the dequenching of effluent dye has been converted to the number of pore openings over the course of time. All the resulting curves exhibit a pronounced slowing down of the pore formation rate revealing two distinct relaxation steps at about 20 and 200 s, respectively, being largely independent of vesicle type and peptide to lipid ratio. The pore formation rate itself increases in proportion to the amount of membrane bound peptide. We give a quantitative account of our experimental findings based on a novel reaction scheme applicable to any of our various liposome systems. It implies that the pore formation rate is controlled by a passage through two intermediate monomeric peptide states. These states are thought to become well populated in the initial stage of lipid bilayer perturbation, but would practically die out after some time owing to a restabilization of the membrane system.

Melittin, the main constituent of bee venom (*apis mellifera*), is a peptide of 26 amino acid residues. Its structural properties and actions on lipid membranes have already been explored on a fairly large scale (see review by Dempsey (1990)). In particular, an α-helical conformation of the given amphipathic amino acid sequence would give rise to segregated hydrophobic and hydrophilic faces. Bundles of such lipid bilayer spanning helices are believed to make up the basic architecture of a protein mediated membrane channel ("barrel-stave" model). Accordingly, studying amphipathic peptides as possible pore formers has attracted considerable interest (see review by Sansom, 1992).

A multitude of relevant natural and synthetic peptides have been shown to cause permeabilization of lipid vesicles. This phenomenon could be monitored experimentally by recording the efflux of an initially entrapped marker substance, preferentially a self-quenching fluorescent dye, for instance CF[1] (Weinstein et al., 1977) which tends to form nonfluorescent dimers (Chen & Knutson, 1988), or a fluorophor−quencher pair, such as ANTS/DPX (Ellens et al., 1984). A peculiar feature of the observed leakage process is its transient nature. Generally there is a drastic slowing down of efflux until it becomes practically terminated, usually leaving the depletion of marker content incomplete.

In order to gain a better insight into the relevant molecular mechanisms, the measured signals should be related to a reasonable physicochemical model of the underlying scheme of reactions. Useful information can be obtained by examining the mode of efflux. It has been characterized as "all-or-none" if individual liposomes have either retained all their marker content or lost it totally. This is indicated by a lack of dequenching of dye remaining inside the vesicles. Such an event was reported with diverse membrane active agents such as apolipoprotein (Weinstein et al., 1981), the peptide GALA (Parente et al., 1990), magainin 2a (Grant et al., 1992), the toxic protein α-hemolysin (Ostolaza et al., 1993) and the neurotoxic peptide pardaxin (Rapaport et al., 1996). A mode of graded efflux (Liu et al., 1988) would be reflected by an internal transient quenching that is gradually reduced over the course of time due to a distribution of partially depleted liposomes. Matsuzaki et al. (1994) have observed this for magainine 2 acting on egg PC−LUV. Pertinent theoretical approaches to evaluate the measured data with appropriate marker substances have been developed for a self-quenching dye (Schwarz & Arbuzova, 1995) as well as for the two-component ANTS/DPX marker system (Ladokhin et al., 1995).

Usually peptide induced leakage has been attributed to the formation of pores. Rather extensive studies were conducted

† This work has been supported by the Grants 31-32188.91 and 31-42045.94 from the Swiss National Science Foundation.

* Corresponding author. Phone: +41 (61) 267 2200. Fax: +41 (61) 267 2189. E-mail: schwarzg@ubaclu.unibas.ch. Department of Biophysical Chemistry, Biocenter of the University of Basel, Klingelbergstr. 70, CH 4056 Basel, Switzerland.

‡ Present address: Department of Biochemistry, McGill University, 3655 rue Drummond, Montreal H3G 1Y6, Quebec, Canada.

[1] Abbreviations: ANTS, 8-aminonaphthalene-1,2,3-trisulfonic acid; CF, 5(6)-carboxyfluorescein; DLS, dynamic light scattering; DOPC, 1,2-di-oleoyl-*sn*-glycero-3-phosphatidylcholine; DOPE,1,2-di-oleoyl-*sn*-glycero-3-phosphatidylethanolamine; DPX, *p*-xylylenebis[pyridinium bromide]; EDTA, ethylenediaminetetraacetic acid; HEPES, *N*-(2-hydroxy-ethyl)piperazine-*N*′-2-ethanesulfonic acid; HPLC, high-performance liquid chromatography; LUV_{100}, large unilamellar vesicles of 100 nm diameter; LUV_{200}, large unilamellar vesicles of 200 nm diameter; NBD, *N*-(7-nitrobenz-2-oxa-1,3-diazol-4-yl); PC, phosphatidylcholine; POPC, 1-palmitoyl-2-oleoyl-*sn*-glycero-3-phosphatidylcholine; SUV, small unilamellar vesicles.

S0006-2960(97)01009-X CCC: $15.00
Published on Web 02/04/1998

with magainin (Matsuzaki et al., 1989; 1991; 1994) and pardaxin (Shai et al., 1990, 1991; Rapaport & Shai, 1991). In their work with the synthetic peptide GALA, Parente et al. (1990) proposed a theoretical model of the molecular mechanism that fits their data but requires irreversible binding of the pore-forming agent. There are, however, systems (e.g., the present one) where the binding is definitely reversible and fast. Nevertheless the leakage may still be incomplete as seen for the effect of magainin 2a by Grant et al. (1992). These authors conclude that pore activation is only feasible during a transient destabilization of the vesicle membrane caused by peptide−lipid interactions. Apparently this also involves a fast lipid flip-flop (Fattal et al., 1994). On the other hand, Matsuzaki et al. (1995a,b) have demonstrated a correlation of pore activation and translocation (of magainin) across the bilayer.

In the present article we provide a comprehensive quantitative examination of CF leakage out of diverse vesicle types to which melittin had been added. Although the lytic effect of this peptide has been known for some time (Yanni et al., 1986), many questions with regard to the underlying molecular mechanism remained unanswered.

Our efforts are directed to resolve the empirical fluorescence signal in terms of the actual pore formation rate. A "pore" is simply taken to be a localized structural defect in the lipid bilayer facilitating ready diffusion of hydrophilic material. We have applied a previously developed theoretical procedure (Schwarz & Robert, 1990, 1992) that involves a parameter quantifying the precise degree of graded efflux (Schwarz & Arbuzova, 1995). The apparent decrease of the observed pore formation rate could then be expressed as a sum of two exponential time functions. We will discuss this finding in relation to the ratio of bound peptide per lipid. Finally, we propose a basic pore-forming mechanism and its rate-limiting steps that describe our experimental results quite satisfactorily. Different vesicle systems were used varying in size and lipid composition in order to determine how pore formation possibly depends on these properties.

MATERIALS AND METHODS

Substances. The buffer (pH 7.4, 20 °C) was composed of 10 mM HEPES (from Bioprobe, Chemie Brunschwig AG, Basel, Switzerland), 107 mM NaCl, 1 mM $Na_2EDTA{\cdot}2H_2O$ (both supplied by Merck, Darmstadt, Germany) and the necessary amount of 5−6 mM NaOH.

The fluorescent dye CF (mixed isomers, $M_w = 376$, 99% pure by HPLC) was obtained from Sigma Chemical Co. (St. Louis, MO). An aqueous stock solution being isoosmolar with the buffer, was prepared of 50 mM CF with 10 mM HEPES, 10 mM NaCl, 1 mM $Na_2EDTA{\cdot}2H_2O$, and some 134 mM NaOH in order to adjust a pH of 7.4 at 20 °C. We determined the concentration of CF by UV spectroscopy at 492 nm using an absorption coefficient of 72000 M^{-1} cm^{-1} (Barbet et al., 1984). The dye solution was stored at 4 °C in the dark.

We purchased synthetic melittin ($M_w = 2840$) from Bachem Feinchemikalien (Bubendorf BL, Switzerland) and used it without further purification. The concentration of the aqueous stock solutions of melittin was determined by UV spectroscopy at 280 nm using an absorption coefficient of 5570 M^{-1} cm^{-1} (Quay & Condie, 1983).

The lipids POPC, DOPC, and NBD−DOPE were obtained in chloroform from Avanti Polar Lipids, Inc. (Birmingham, AL). They have been used without further purification. Their concentration was measured through phosphate analysis (Böttcher et al., 1961).

Lipid Vesicles. The preparation of SUV by ultrasonic irradiation and LUV by extrusion (Mayer et al., 1986), with and without CF, has been carried out as described in detail elsewhere (Schwarz & Arbuzova, 1995; Rex, 1996). Prior to all experiments, the external dye was separated from the vesicles by gel filtration over a Sephadex G50 column (1 × 30 cm, Pharmacia, Uppsala, Sweden) using a detection wavelength of 490 nm.

According to reports in the literature about 10−25% of multilamellar vesicles have been observed after extrusion of LUV_{200} (Hope et al., 1986; Mayer et al., 1986). However, freeze−fracture electron microscopy indicated only negligible amounts of such artifacts in our studies (B. Sternberg and S. Rex, unpublished results).

We determined by DLS the hydrodynamic radius of SUV as 12(±1) nm and that of LUV_{100} as 53(±3) nm as reported previously (Rex, 1996). For LUV_{200} we obtained analogously a radius of 120(±10) nm. On the basis of the geometric requirements in a PC vesicle bilayer (Huang & Mason, 1978) we can then calculate the number of lipid molecules per vesicle (Rex, 1996) to be $N_L \approx 5.3 \times 10^5$, 9.8×10^4 and 3.5×10^3 for LUV_{200}, LUV_{100}, and SUV, respectively.

Generally, liposome preparations of any kind are difficult to be reproduced at high quality in the same physical state. This is apparently due to their metastable nature implying a certain variability of structural defects in the lipid bilayer which affect binding and leakage properties. Accordingly, we must take into account some scattering of the measured data in our diverse experiments. We have therefore averaged the results over a larger number of reiterated vesicle preparations. This leaves an inherent uncertainty margin which will be indicated at the respective places.

Binding Experiments. Association of melittin with the differently sized POPC and DOPC liposomes was determined by a resonance energy transfer assay that has been developed in our laboratory (Hellmann & Schwarz, 1997). All vesicles contained 0.3 mol % of NBD−DOPE. Energy transfer between the tryptophane (donor) of bound melittin and the NBD (acceptor) in the polar headgroup of the DOPE was measured as enhanced NBD emission. It turned out to be quite efficient to yield a useful binding signal. We used a Jasco FP 777 spectrofluorometer (Japan Spectroscopic Co., Tokyo) with excitation at 280 nm (slit 1.5 nm), emission at 530 nm (slit 3 nm), and a cutoff filter at 295 nm. The 1 × 0.5-cm quartz cuvettes were kept at 20 °C. To obtain the binding isotherms, we added successively small volumes (ranging from 4−100 μL) of the vesicle stock solution (10mM) to a solution of 1 mL buffer containing 4−10 μM peptide. It is advisable to add vesicles to the peptide−buffer solution rather than vice versa, as vesicles are in this way titrated with higher reproducibility and the peptide concentration can so be controlled quite easily.

The fluorescence signal reflecting binding was recorded within a few seconds after mixing. There was no further change indicative of additional slow binding (e.g., due to a translocation process of melittin towards the inner membrane

leaflet). We corrected the measured value for the contributions of buffer and lipid (which was titrated separately). Contributions from the peptide could be neglected. A correction for the light scattering of the vesicles has also been taken into account as proposed by Hellmann and Schwarz (1998). It provides the signal to be processed toward a binding curve (see below in Results and Discussion).

Efflux Measurements. The experiments were performed with excitation at 480 nm (slit 1.5 nm), emission at 518 nm (slit 5 nm), and a cutoff filter at 495 nm. The 1 × 1-cm quartz cuvettes contained a final volume of 2 ml of buffer and vesicles filled with the fluorescent dye at a self-quenching concentration (being continuously stirred at 20 °C). In this state we measured the initial fluorescence signal F_o before adding the melittin. The concentrations of lipid ranged from 20 to 280 μM, those of the peptide from 0.004 to 5 μM.

We followed the increasing fluorescence signal $F(t)$ within 20 min. The signal F_∞ (for all dye being released at $t \rightarrow \infty$) was determined after the addition of about 50 μL of a 10% (w/w) solution of Triton X-100 (from Merck, Darmstadt, Germany) causing complete lysis of the vesicles. The F_o- and F_∞-values have been corrected for dilution due to the addition of the melittin and Triton X-100 stock solution volumes, respectively. The originally recorded signal $F(t)$ has always been normalized to an empirical efflux function

$$E(t) = (F_\infty - F(t))/(F_\infty - F_o) \qquad (1)$$

which describes the time course of the fluorescence signal and reflects the leakage process under consideration. It is, however, not necessarily in proportion to the actual percentage of dye release (see below).

The spontaneous efflux rate of the LUV (measured with vesicles suspended in pure buffer) could be easily neglected. It was at least an order of magnitude below the level observed under any conditions for the melittin-induced leakage. In the case of the SUV, the slow steady-state rates were at a minimum of 0.35% fluorescence intensity change per minute, increasing to some 4% at our largest bound peptide to lipid ratios, by contrast to about 0.1−0.2% for the spontaneous leakage. Under the given circumstances we have neglected this, too. We feel encouraged to do so also by experimental evidence that the SUV are to some degree protected against their comparatively large spontaneous efflux by some action of the bound peptide. This is founded on observations in our laboratory that after 1−2 h peptide-infected vesicles have lost distinctly less dye than uninfected ones (Arbuzova, 1996).

Quenching Factors. We determined the self-quenching efficiency of vesicle entrapped dye under static conditions. A number of dye solutions were prepared by dilution of our 50 mM CF stock solution with buffer. Each solution was entrapped into vesicles (SUV, LUV_{100}, and LUV_{200}) consisting of either POPC and DOPC lipid, respectively. The vesicles were given into a buffer containing cuvette resulting in a total volume of 2 mL. Having recorded the F_o-value of the vesicles we then added 20 μL Triton X-100 (10%-w/w) to determine the F_∞-value. Subsequently, the static quenching factor $Q_o = F_o/F_\infty$ was calculated, taking the average of three independent measurements. Because of the spontaneous efflux, especially in the case of the SUV, the measurements of Q_o were carried out immediately after separation of external CF from the vesicles by gel filtration.

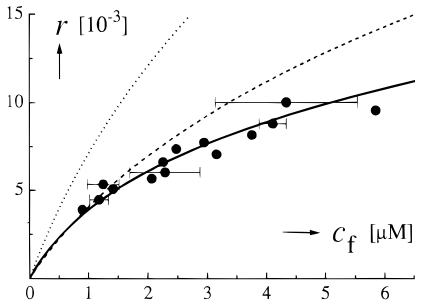

FIGURE 1: Association isotherms expressing the ratio of bound melittin per lipid r versus the free peptide concentration c_f. The data points apply to the system POPC−LUV_{200}. Their possible scattering as observed for reiterated vesicle preparations (see text) is indicated by the selected error bars. The solid curve is a best fit for the averaged points according to the eqs 2a,b using $b = 11.5$ (for the present ionic strength) and $K_p = 6 \times 10^3$ M^{-1}, $z = 2.2$. Analogously, the dashed and dotted curves fit our data (not shown for clarity) with POPC−LUV_{100} and POPC−SUV, respectively. In these and all our other curve fittings we used a software built-in Marquardt−Levenberg algorithm. The goodness of fit was optimized by a least-squares minimization.

On the other hand, we modified the ordinary efflux runs so that transient quenching factors could be determined (Schwarz & Arbuzova, 1995) with a volume of 2.5−3 mL buffer containing dye loaded vesicles and melittin. Each experiment has been conducted under the condition that the efflux has practically stopped at some degree of incomplete depletion, indicated by a certain value of the fluorescence signal $F(t)$ that is equivalent to an intermediate efflux function $E(t)$. In the case of the LUV we simply waited for the final slow phase, with the SUV we also created an immediate termination of the efflux by adding a 6−12 times excess of empty vesicles. Then a volume of 0.8−1 mL, taken out of the cuvette, was subjected again to gel filtration to be separated from the so far released dye and the melittin. With the latter vesicle sample in a clean cuvette, we recorded its signals F_o* and F_∞*, taken before and after an addition of sufficient Triton X-100, respectively. The appropriate transient quenching factors $Q_t = F_o*/F_\infty*$ were registered in relation to the respective efflux function $E(t)$ (which refers to the same time instant of the efflux process) and compared with the initial Q_o. By measuring the fluorescence emission of the column eluent we checked that the column was free of CF before injecting the next sample. A constant signal F_o* confirms the absence of peptide that could possibly induce further efflux.

RESULTS AND DISCUSSION

Association Isotherms. The corrected signal in our fluorescence energy transfer assay (see above) was registered at a series of the given total peptide concentration c_P upon a titration with unloaded liposomes while gradually increasing the total lipid concentration, c_L. The pertinent method of data processing toward a "binding curve" has been described in great detail elsewhere (Schwarz et al., 1987; 1997; Schwarz & Beschiaschvili, 1989; Schwarz, 1996). It provides a model-free access to the association isotherm, being expressed as bound peptide per lipid, r, versus the free peptide concentration, c_f. In Figure 1 we present an example

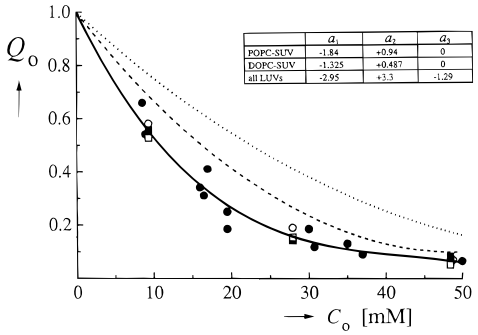

FIGURE 2: Static quenching factor Q_o of vesicle-entrapped CF versus the internal dye concentration c_o. The data points apply to POPC−LUV_{200} (○), POPC−LUV_{100} (●), DOPC−LUV_{200} (□), and DOPC−LUV_{100} (■), respectively. They are fitted by the solid curve according to eq 4. Analogous fits (data points not shown for clarity) are given for POPC−SUV (dashed curve) and DOPC−SUV (dotted curve). The appropriate coefficients are presented in the inset. The data for POPC−LUV_{100} and POPC−SUV have been adopted from Schwarz & Arbuzova (1995).

for the special case of melittin associated with POPC−LUV_{200}. The data points have been averaged over the c_f-values at a series of certain r-levels, usually taken from four to six different titrations.

The association is most reasonably described in terms of a partitioning process of the peptide between a two-dimensional solvent (the lipid bilayer) and the aqueous bulk phase. There are no specific binding sites. Nevertheless we may use the popular term "binding" (in a more general sense) as a possible synonym for "association". As pointed out previously (Schwarz & Beschiaschvili, 1989) one can under equilibrium conditions derive the relations

$$r = (K_p/\alpha)c_f, \quad \ln \alpha = 2z \sinh^{-1}(zbr) \qquad (2a,b)$$

where K_p stands for the appropriate partition coefficient (being independent of concentrations) and α is an activity coefficient which by virtue of a Gouy−Chapman model approach can be expressed in terms of the effective charge number per monomer z and a parameter b depending on the ionic strength in the aqueous moiety. The eqs 2a,b have been applied to fit curves to the data, as demonstrated in Figure 1. The respective pairs of K_p and z that were in this way determined for our various vesicle systems are compiled in Table 1. Owing to the inevitable scattering of the data points, an uncertainty of up to ±30% in K_p and 15% in z may be involved (however, the possible high and low extremes of K_p would go along with about 20% higher and lower values of z, respectively).

The ratio of membrane associated peptide per lipid r should naturally be a controlling parameter of the leakage effect. This is, however, not unambiguously so with the overall peptide-to-lipid ratio, c_P/c_L, which is a rather popular parameter since it can be quite easily adjusted in the laboratory. Nevertheless it must be emphasized that, in a partitioning equilibrium, the same value of c_P/c_L allows for variable values of r depending on the magnitude of the given c_L. By all means, the fraction of bound peptide will increase if a higher lipid concentration is used. In other words, one may observe divergent leakage effects with the same c_P/c_L at different vesicle concentrations.

We have characterized our melittin−vesicle systems by the partition coefficients and effective charge number

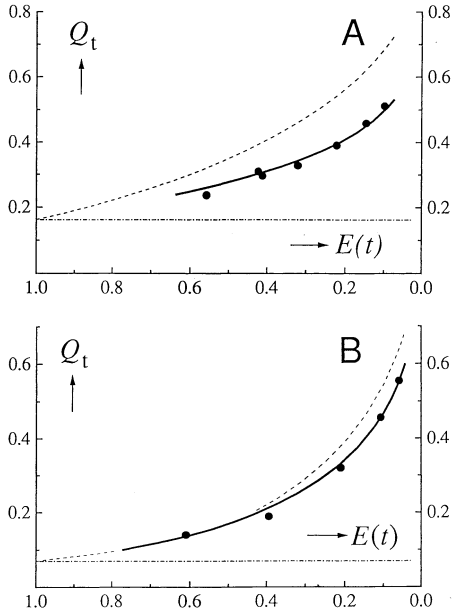

FIGURE 3: Transient quenching factors Q_t versus the measured efflux function $E(t)$. The dotted line and dashed curve refer to the two extreme modes of efflux, $\rho = 0$ and $\rho \to 1$, respectively. (A) Data for POPC−SUV with $Q_o = 0.162$ (initially entrapped c_o = 36 mM). The solid curve was calculated with the eqs 5 and 7 and $\rho = 0.54$. (B) Analogous results for POPC−LUV_{200} with Q_o = 0.070 (c_o = 47.5 mM) and $\rho = 0.83$. Special attention was directed to fit the data points at higher depletion of internal dye (i.e., low $E(t)$) because this involves more significant differences between the two extreme modes (see text).

Table 1: Binding Parameters of the Association Equilibrium (for the Given Ionic Strength of 0.11 M, 20 °C, pH 7.4) According to the Eqs 2a,b (b = 11.5)[a]

lipid species	vesicle size	K_p [10^3 M^{-1}]	z
POPC	LUV_{200}	6	2.2
	LUV_{100}	5	1.5
	SUV	9	1.2
DOPC	LUV_{200}	5	1.6
	LUV_{100}	7	1.3

[a] Uncertainties are estimated to be about ±30% for K_p and ±15% for z (see text for comment).

presented in Table 1. In the case of melittin-induced leakage as studied in this work we deal with very low values of r ($<\approx 10^{-3}$) so that practically $\alpha = 1$. Thus "ideal" partitioning can be presumed with $r = K_p c_f$, applying to the initially linear part of the association isotherms (see Figure 1 at $c_f < \approx 0.3\ \mu M$). By means of mass conservation eq 2a may then be converted into

$$r = x_{as}(c_P/c_L), \quad x_{as} = K_p c_L/(1 + K_p c_L) \leq 1 \qquad (3)$$

We have generally employed conditions with a considerable percentage of free peptide. In the special case of POPC−LUV_{200} (see Figures 4 and 5) c_P/c_L varies between 6×10^{-5} and 1.6×10^{-3} (c_L ranges from 20 to 60 μM). The molar fraction of bound peptide x_{as} then falls within 10−30%. Accordingly, only a minor part of the added melittin is associated with the membrane. In fact, if we add some more dye-loaded liposomes, another burst of marker release occurs revealing the presence of a sufficient amount of free peptide. The latter undergoes a fast exchange with the bound one in the millisecond range as has been demonstrated by stopped−

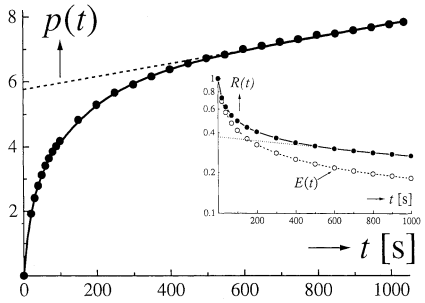

FIGURE 4: Number of activated pores per vesicle $p(t)$ in the course of time t evaluated from the normalized change of the fluorescence signal $E(t)$ for a special experiment with POPC−LUV_{200} where we had $c_o = 44.5$ mM CF, $c_P = 0.018$ μM, $c_L = 0.44$ μM, and $r = 8.43 \times 10^{-5}$ (corresponding to a molar fraction of bound melittin $x_{as} = 0.206$). The solid fit curve of $p(t)$ is calculated according to eq 9b using the kinetic parameters (given in 10^{-2} s^{-1}) v_1, 11.2; v_2, 2.47; v_3, = 0.02; k_1, 5.4; k_2, 0.67. The dashed straight line reflects the slow linear increase of pore openings in an apparent steady state after a few minutes.The inset displays semilogarithmic plots of the fluorescence change in terms of $E(t)$ (indicated by open circles) and the actual decrease of entrapped dye content, expressed by $R(t)$, as calculated by means of the eqs 5 and 7 ($Q_o = 0.078$, $\rho = 0.83$). The dotted line marks an exponential time course encountered under the final steady-state conditions.

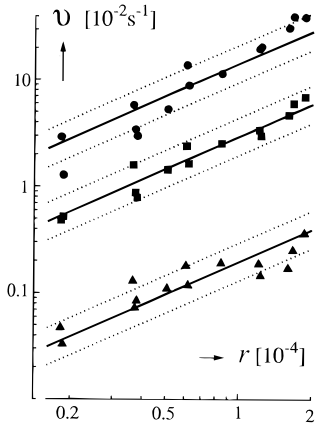

FIGURE 5: Double logarithmic plots of the three rate amplitudes, v_1 (●), v_2 (■), and v_3 (▲) as a function of the associated peptide to lipid ratio r, determined for the POPC−LUV_{200} system. The straight lines correspond to first-order rate laws. The slopes of the solid lines have been used to derive the appropriate values of v^* in Table 3 (the dotted lines refer to deviations by ±50%).

flow experiments (Schwarz & Beschiaschvili, 1989; Sekharam et al., 1991). We have confirmed this by observing an immediate termination of efflux upon adding an excess of unloaded vesicles, indicating a rapid redistribution of associated melittin resulting in an insufficient peptide-to-lipid ratio on the loaded liposomes.

Our results do contrast with those of Benachir and Lafleur (1995) who reported for the POPC−LUV_{100} system the absence of free peptide at a minimum requirement of $c_P/c_L \approx 2 \times 10^{-3}$ (≅r) in order to induce efflux. However, we have measured appreciable marker release already below $r = 10^{-4}$. Additionally (Rex, 1995), when adopting their somewhat different efflux conditions (i.e., calcein instead of CF, natural melittin, higher salt concentrations), we still found discrepancies in the efflux behavior (see below), which could not be explained satisfactorily at present.

The observed r-data are easily converted to the number of bound peptide monomers per vesicle by multiplication with N_L (see Materials and Methods). It turns out that a very small number of molecules on the vesicle membrane can nevertheless induce marker release. In the case of POPC−LUV_{100}, we have seen this with an average of only four (!) bound monomers in contrast to the system of Benachir and Lafleur (1995) where more than a hundred are apparently needed. By all means, we conclude from our data that efflux definitely occurs already in cases where only about 0.1−1% of the vesicle surface is covered by peptide. This suggests the existence of pore formation at isolated spots rather than an increase of permeability spread out evenly over the bilayer.

Mode of Efflux and Pore Lifetimes. In order to evaluate the fluorescence signal in efflux experiments with a self-quenching fluorescent marker, the extent of quenching has to be determined quantitatively under static and transient circumstances in terms of the quenching factors Q_o and Q_t, (see Materials and Methods). In Figure 2 we present Q_o as it depends on c_o (i.e., the concentration of entrapped dye). The fit curves shown in the figure have been calculated using an *empirical* third power polynomial, namely

$$Q_o(c_o) = 1 + a_1 y + a_2 y^2 + a_3 y^3 \qquad (4)$$

where $y = c_o/50$ mM. The fits are supposed to apply up to $y = 1$. This will be used in the theoretical analysis discussed below.

The transient quenching factor Q_t measures the average dequenching of the entrapped dye after the peptide induced leakage was started. With this quantity the experimental efflux function $E(t)$ can be converted to a retention function

$$R(t) = [(1 - Q_o)/(1 - Q_t)]E(t) \qquad (5)$$

that is equal to the fraction of the original marker content being still retained in the vesicles (Schwarz & Arbuzova, 1995). Thus the change of the fluorescence signal does not simply reflect the true amount of dye having leaked out of the liposomal interior unless we deal with an "all-or-none" mode of efflux (where $Q_t = Q_o$ remains constant).

Once a mode of graded efflux is effective, Q_t will increase along with the release of dye, implying $R(t) > E(t)$. In a quantitative analysis of such a situation, however, a reasonably precise description of the actual degree of graded efflux beyond the "all-or-none" case will be needed. In a basic theoretical model of pore formation (assuming noninteracting uniform pores) this has been expressed in terms of a single-pore retention factor ρ (i.e., the average fraction of marker content retained inside a vesicle if just one pore had been open (Schwarz & Robert, 1992)). The release of marker through a single pore follows an exponential time function involving a relaxation time τ_o (Schwarz & Robert, 1990). In the case of the limited size of our vesicles, this τ_o is expected to be in the subsecond range. Then $\rho(t)$ would become independent of time and can be expressed as

$$\rho = \tau_o/(\tau_o + \tau_p) \qquad (6)$$

where τ_p stands for the average lifetime of a pore opening. In this model the extent of graded efflux, described by the parameter ρ, may thus be related to the ratio τ_p/τ_o, being a reduced measure of the pore lifetime. Accordingly "all-or-none" is equivalent to $\rho = 0$, in other words the first pore is

Table 2: Single Pore Retention Factors ρ for the Melittin−CF Vesicle Systems Determined from the Measurements of the Transient Dequenching Effect[a]

	POPC	DOPC
SUV	0.54 (0.85)	0.57 (0.75)
LUV_{100}	0.91 (0.10)	0.79 (0.27)
LUV_{200}	0.83 (0.20)	0.89 (0.12)

[a] Uncertainties are estimated to be about ±0.05. The average pore lifetime in proportion of the relaxation time of the efflux through a single pore τ_p/τ_o according to eq 6 is given in parentheses.

sufficiently long-lived to allow total depletion of the entrapped dye in any infected liposome. The opposite extreme would be $\rho \rightarrow 1$, which corresponds to an evenly decreasing level of marker in all the liposomes because of very short pore lifetimes so that a multitude of pore openings is required.

In an extension of this theory the experimentally accessible value of Q_t can be related to the factor ρ and the parameters of equation 4 through the equation

$$Q_t = 1 + \sum_m a_m \cdot y^m [R(t)]^{z_m} \qquad (m = 1, 2, 3)$$
$$\text{where } z_m = m\rho/(m + 1 - m\rho) \quad (7)$$

[see the detailed account by Schwarz and Arbuzova (1995)]. Together with equation 5 the appropriate Q_t at any observed value of $E(t)$ may so be calculated for a given $\rho < 1$.

In view of this approach we have plotted our measured Q_t versus the respective value of $E(t)$ as shown for the two examples in Figure 3. Evidently the data points can quite satisfactorily be fitted by a solid curve corresponding to a specific ρ-value. The resulting numbers for our diverse vesicle systems are collected in Table 2. All of them clearly indicate a mode of substantially graded efflux.

The true percentage of release must be determined from the measured fluorescence changes in terms of the efflux function $E(t)$ through the retention function $R(t)$ as expressed by equation 6. This requires knowledge of the transient quenching factor Q_t over the entire range of $E(t)$. In view of the scissors-like opening of possible Q_t values between the extreme values Q_o and that for an even leakage rate of all vesicles, a clear-cut increase of Q_t (reflecting more or less graded efflux) may possibly only be observed at a rather high extent of the overall efflux (see the situation in the Figure 3A,B). Such a predicament could particularly be encountered at a rather high entrapped dye concentration where the static quenching factor remains largely invariant over wide range of c_o (as it applies for example to CF at concentrations beyond about 50 mM). Under these circumstances one may mistakenly infer the existence of an "all-or-none" mode of efflux from a measured Q_t remaining approximately equal to Q_o at an insufficient extent of efflux. This aspect has apparently been overlooked in a previous analysis of melittin and POPC−SUV (Schwarz et al., 1992) where an "all-or-none" mode was proposed. Now we could demonstrate that our data can be very well described up to a high degree of marker release (i.e., $E(t) < 10\%$) by assuming a graded efflux mode. Thus equation 5 may be readily applied in order to calculate $R(t)$.

In contrast to our findings of a graded release Benachir and Lafleur (1995) determined an "all-or-none" mode for melittin under their chosen experimental conditions. We note that the wasp venom factor mastoparan X (a smaller but structurally similar peptide) was found to make POPC−LUV leaky in a graded mode, whereas small unilamellar POPC vesicles were emptied by an "all-or-none" mode (Schwarz & Arbuzova, 1995). Further relevant reports in the literature have been enumerated in the introduction. These examples indicate that the mode of dye release is not only determined by the properties of the considered agent and its membrane interactions but also by the chosen experimental conditions such as the lipid composition of the membrane, vesicle size, pH, and salt concentration.

According to equation 6 the parameter ρ is controlled by τ_p/τ_o (i.e., the ratio of the average pore lifetime and the relaxation time of marker release through a single pore). For our diverse melittin−vesicle systems these quantities are specified in Table 2. We may now estimate the average duration of a pore opening. The magnitude of τ_o depends on the pore structure and should be proportional to the internal vesicle volume (Schwarz & Robert, 1990). The case of LUV_{200} (internal radius ≈ 116 nm) and a possible pore diameter of 1.5 nm allows a $\tau_o \approx 30$ ms so that $\tau_p \approx 6$ ms. In the other cases even smaller lifetimes can be estimated. Therefore an open pore may be a comparatively very short-lived event. Accordingly the probability that a bound peptide resides in an active pore state remains extremely small. Consider for instance that even for the most unfavorable case of the initial fast rate the number of pore openings is always less than 0.1 per 10 bound peptides during a measuring time $\Delta t = 1$ s. Even if 10 monomers should be involved in an active pore, the average fraction of monomeric pore states would therefore be equal to $\tau_p/\Delta t < 1\%$.

Pore Formation Rates. In each individual dye release experiment we have recorded the efflux function $E(t)$ and then converted it to the appropriate retention function $R(t)$ by applying the equations 5 and 7 with the appropriate ρ-factor. As demonstrated in the inset of Figure 4, the true extent of dye efflux $R(t)$ may appreciably deviate from the apparent normalized change of the fluorescent signal $E(t)$. It can also be seen that after a few minutes the initially very fast leakage process will slow down dramatically (by about 2 orders of magnitude). $R(t)$ can then be described by a single exponential time function (see the dotted line in the inset of Figure 4).

The average number of pore openings per vesicle $p(t)$ in a time interval t (after having started the release process) has been evaluated by means of the relation

$$p(t) = -(1 - \rho)^{-1} \ln R(t) \qquad (8)$$

(Schwarz & Robert, 1992). An example is shown in Figure 4. The slope $v = dp/dt$ would be equal to the pore formation rate per vesicle. The very drastic slowing down during a period of a few minutes can be very well described by two clearly separated relaxation terms according to

$$v(t) = v_1 \exp(-k_1 t) + v_2 \exp(-k_2 t) + v_3 \qquad (9a)$$

as already observed with the similar case of the wasp venom peptide mastoparan X (Arbuzova & Schwarz, 1996). This includes a constant slow rate v_3 when an apparent steady state of pore formation is eventually reached. By integration of $v(t)$ we obtain

$$p(t) = (v_1/k_1)[1 - \exp(-k_1 t)] + (v_2/k_2)[1 - \exp(-k_2 t)] + v_3 t \quad (9b)$$

The $p(t)$ versus t data have accordingly been fitted (see Figure 4). Such an excellent fit was obtained in any individual case of a given vesicle preparation so that the various kinetic parameters k_1 and k_2, as well as v_1, v_2, and v_3, could be determined quite well. However, because of the already indicated limited reproducibility of vesicle preparations, we encounter again some variabilitity of these parameters in our measuring series. The results are then examined by means of double-logarithmic plots versus the appropriate concentration variable of bound melittin r (using the partition coefficients of Table 2 with the same K_p for both SUV-systems). This is done with regard to a possible integer slope reflecting an underlying order of reaction.

The observed time constants k_1 and k_2 reveal no significant changes upon raising r within the scope of the unavoidable scattering of the data. Thus we conclude that these time constants remain constant. Our results (averaged as ln k) are given in Table 3. They reflect two relaxation steps at about 20 and 200 s, respectively.

In Figure 5 double-logarithmic plots of each of the three rate amplitudes v_1, v_2, and v_3 versus r are presented for the same POPC−LUV_{200} system. There is a significant increase when r is raised. In view of the inherent uncertainties, straight lines with slope one fit the data best. In other words, a first-order rate law (i.e., a proportionality to r) turns out to be consistent with any of the three rate amplitudes. Analogous features have been observed with the other vesicle systems. We may therefore characterize the diverse rate amplitudes by their particular constant slope values v/r.

In order to compare pore activities on vesicles of different sizes, v should be divided by N_L. The reduced rate $v^* = v/rN_L$ then becomes equal to the rate of pore openings per bound peptide monomer. It will be independent of r. For the sake of relating our results to a possible molecular mechanism, we collected the averages of three characteristic reduced rate amplitudes in Table 3. These are v_0^* (derived from extrapolated initial rate $v_0 = v_1 + v_2 + v_3$ at $t = 0$), the intermediate v_i^* (measuring $v_2 + v_3$) and the final steady-state value v_∞^* (related to v_3 at $t \rightarrow \infty$).

Molecular Mechanism of Pore Formation. A quantitative analysis of our experimental results may be attempted with regard to the rate limiting steps in the underlying scheme of reactions. To this end we shall first emphasize a number of points that have to be taken into account: (i) A substantial part of the peptide remains free in the aqueous moiety. It permits a fast exchange of the pore forming agent between the lipid vesicles. This rules out that the slowing down of marker efflux results from irreversible peptide binding.

(ii) The amount of bound peptide remains practically constant during the leakage process (indicated by the observed lack of a slow change of the binding signal). The bound peptide is predominantly in a monomeric state, presumably adopting a kind of wedgelike position on the bilayer surface (Dempsey, 1990).

(iii) The pore appears to be very short-lived so that at any given instant the amount of bound peptide actually participating in a pore opening would be negligibly small.

Table 3: Averages of Pore-Forming Rate Parameters for the Various Melittin−Vesicle Systems According to the Eqs 9a,b (Experimental Uncertainties are around 20−50%)[a]

vesicle systems	k_1 [10^{-2} s^{-1}]	k_2	v_0^*	v_i^* [10^{-5} s^{-1}]	v_∞^*
POPC−LUV_{200}	5.0	0.65	320	59	3.8
−LUV_{100}	5.0	0.50	980	230	17
SUV	6.0	0.45	250	36	6.5
DOPC−LUV_{200}	12.5	0.70	110	8.4	0.8
−LUV_{100}	10.5	0.65	170	16	1.5
SUV	6.5	0.60	210	27	3.4

[a] The $v^* = v/rN_L$ stand for a reduced rate per bound peptide monomer (see text).

(iv) Upon adding the peptide the lipid bilayer will be subject to a fast perturbation with an apparent lipid flip-flop (Fattal et al., 1994). This should offer an opportunity for peptide monomers to penetrate farther into the bilayer permitting better possibilities to create a pore. A restabilization of the peptide−lipid arrangement in the membrane may then lead to drastically reduced probabilities of these favorable monomeric states.

(v) The first-order characteristics of the pore-formation rates, as observed in our experiments, suggest the existence of a nucleation step involving a passage through two rate-limiting intermediate monomeric states.

In view of these aspects we propose the following scheme (Scheme 1) of reactions

Scheme 1

$$A_{free} \overset{fast}{\rightleftharpoons} A_0 \underset{k_{10}}{\overset{k_{01}}{\rightleftharpoons}} A_1 \underset{k_{21}}{\overset{k_{12}}{\rightleftharpoons}} A_2 \xrightarrow{k_{23}} A_3 \xrightarrow[(+mA)]{fast} pore \rightarrow X$$

The respective first-order rate constants indicated are to apply when the efflux is actually being measured (i.e., after the initial perturbation period). The A_0 stands for the main binding state of monomers, which is always coupled with the free monomer A_{free} through a fast partitioning equilibrium. The states A_1 and A_2 are seen as bound monomers in a structurally and/or energetically more favorable penetrating position. These states are envisaged to become reasonably well populated during the initial perturbation period. The step $A_2 \rightarrow A_3$ then results in a monomeric nucleus which immediately undergoes a reaction toward a pore opening, possibly together with m additional monomers. How many such monomers are actually needed is not at all clear. As far as our present study is concerned, we can only conclude that monomeric states form some kind of rate-limiting pore nuclei. Thus we must not generally rule out a possible lipidic pore being induced by a peculiar melittin monomer. Nevertheless the idea of a peptide aggregate appears to be more appealing as it is indeed largely favored in the literature. The number of monomers per pore is at any rate uncertain, however. It may be as low as 2−4 (Fattal et al., 1994) but could be, according to estimations based on apparent pore sizes, even 6−20 (Rex, 1996) or 10−15 (Ladokhin et al., 1997). Anyway, in our model the relevant rate of pore openings would be determined by the production rate of A_3. This implies

$$v = k_{23} N_L r_2 \quad (10)$$

where r_2 denotes the bound peptide/lipid ratio of A_2. The pore is presumed to equilibrate rapidly with the bulk of bound

peptides (as indicated by state X) so that the relevant pore formation and decomposition rates cancel out each other. Furthermore, as pointed out above in point iii, we may neglect in the mass conservation condition all peptides that are momentarily engaged in an active pore. The rate will be determined solely by the variables r_i ($i = 0, 1, 2$) or (i.e., the ratios of bound peptide to lipid in the corresponding states A_i).

Applying common routines of reaction kinetics we may now set up two linear differential equations for the peptide/lipid ratios r_1 and r_2 (to be solved by means of standard mathematical procedures). The resulting time function for r_2 (to be inserted in eq 10) will actually feature two relaxation terms and a steady-state value $\boldsymbol{r}_2$. Because of our experimental findings of two time constants that differ by about 1 order of magnitude, we may introduce the condition

$$k_{01} \ll k_{12}, k_{21} \tag{11}$$

Then the solution of the rate equations can be fairly much simplified (see the more detailed mathematical reasoning in the Appendix). In this way we arrive in fact at a quantitative account of our experimental kinetics. The five rate parameters of Table 3 turn out to be related to the kinetic parameters of Scheme 1 as

$$k_1 = k_{21} + k_{23}, \quad k_2 = k_{10} + k_{12}\cdot(k_{23}/k_1) \tag{12a,b}$$

$$v_0^* = v_1^* + v_2^* + v_3^* = k_{23}\cdot x_{20},$$

$$v_i^* = v_2^* + v_3^* = k_{12}(k_{23}/k_1)x_{10},$$

$$v_\infty^* = k_{23}\boldsymbol{x}_2 \tag{12c,d,e}$$

This involves the initial molar fractions of bound peptide in the states A_1, A_2 ($x_{i0} = r_{i0}/r$) and the final steady-state molar fraction $\boldsymbol{x}_2 = (k_{12}/k_1)\boldsymbol{x}_1$, $\boldsymbol{x}_1 = k_{01}/k_2$. Vice versa, one can calculate the rate constants in the scheme, which are quantitatively consistent with the data collected in Table 3. Generally one obtains

$$k_{23} = v_0^*/x_{20}, \quad k_{21} = k_1 - k_{23}, \quad k_{12} = v_i^*(k_1/k_{23})/x_{10} \tag{13a,b,c}$$

$$k_{10} = k_2 - k_{12}(k_{23}/k_1), \quad k_{01} = v_\infty^*(k_1/k_{23})(k_2/k_{12}) \tag{13d,e}$$

There is, however, some degree of freedom since the possible initial population terms x_{10} and x_{20} may be varied to a certain extent under the condition $x_{10} + x_{20} \leq 1$. Because of the eqs 12a,c, the constraint $x_{20} \geq v_o^*/k_1$ also has to be fulfilled. For x_{10} any value between 0 and $1 - x_{20}$ could then be taken. A numerical example will illustrate our findings for the case of POPC−LUV_{200}. With $x_{20} = 0.07$, $x_{10} = 0.1$ (being nearly the smallest possible values!) this leads to $k_{23} = 4.6 \times 10^{-2}$ s^{-1}, $k_{21} = 4.3 \times 10^{-3}$ s^{-1}, $k_{12} = 6.4 \times 10^{-3}$ s^{-1}, $k_{10} = 6.2 \times 10^{-4}$ s^{-1}, and $k_{01} = 4.2 \times 10^{-5}$ s^{-1}. Note that condition 11 is satisfied. Furthermore, one finds $\boldsymbol{x}_1 = 6.5 \times 10^{-3}$ and $\boldsymbol{x}_2 = 8.3 \times 10^{-4}$.

It appears to be reasonable that only small amounts of bound peptide have initially made it into the states A_1 and A_2 (leaving 83% of bound peptide in A_0 with the above example). In the course of the two relaxation steps, the initial 7% bound peptide in A_2 have accordingly dropped to only 0.08%, whereas 0.65% remain in A_1. Thus the rest of more than 99% is eventually accumulated in the main bound state A_0.

Apparently the membrane bound peptide may somehow aggregate in order to form a pore. In several other cases (e.g., the most recent one with pardaxin (Rapoport et al., 1996)) leakage due to pores have been discussed on the basis of aggregation models. Surprisingly, our findings with melittin reveal rate-determining steps of the first order. Thus aggregation must proceed rapidly enough so that our kinetic data in the seconds and minutes range allow no explicit access to this process. Lateral diffusion in the bilayer would be sufficiently fast for that in any case. It takes a molecule only about 25 ms to cover the largest possible distance (i.e., $\approx 3 \times 10^{-5}$ cm on a LUV_{200}) in the course of random walk (with an expected lateral diffusion coefficient of 10^{-8} cm^2/s). In view of the point that we have observed leakage with a very small average number of bound melittin monomers per vesicle, we should also emphasize the fast exchange of the peptide between the vesicles and the aqueous surroundings. Accordingly each vesicle has good chances to bind many more than the average number of monomers once in a while because of the underlying statistical fluctuation dynamics (subject to a Poisson distribution).

Following common approaches of reaction kinetics we have proposed two monomeric peptide states of low population that play the role of transient intermediates. Naturally they are not easily detected directly. Anyway the above Scheme 1 is the simplest model mechanism which does quantitatively agree with our present knowledge.

Influence of Vesicle Size and Lipid Species. The values of K_p and z of melittin for each of our vesicle systems are summarized in Table 1. In the case of POPC, the association isotherms for increasing vesicle sizes are compared in Figure 1. In the range of peptide concentrations where we did the efflux measurements, there is a slightly higher binding affinity to SUV than to LUV, but practically the same one to LUV_{100} and LUV_{200}. Regarding POPC- and DOPC-membranes we observed no difference at low peptide concentrations. However, at higher peptide amounts an increased binding to DOPC- compared to POPC-vesicles (with the same hydrodynamic radius) was found (data not shown). These findings are reflected in the values of K_p and z.

Differences in binding to POPC- or DOPC-membranes at higher peptide concentrations are obviously caused by different structural features of these lipids. It is known from NMR measurements that melittin exerts a pronounced effect on the head group region of a POPC-bilayer where a conformational change of the phosphocholine headgroup is induced (Kuchinka & Seelig, 1989).

The effect of enhanced binding of melittin and other peptides or proteins to SUV in comparison with LUV has been already a point of discussion in the literature [see Kuchinka and Seelig (1989) and references therein]. An increase of packing density and a decrease of membrane defects cause a weakening of binding which explains our data very well. The differences between SUV and LUV are more striking than those between LUV_{100} and LUV_{200}, indicating that the increase in packing density and the loss of membrane defects are nearly similar for the larger vesicles.

The quenching mechanism of carboxyfluorescein in vesicles has been investigated by Chen and Knutson (1988). They concluded that CF is quenched (i) by a static dimerization process leading to the formation of nonfluorescent dimers

and (ii) by an energy transfer between monomers and dimers. Time-resolved fluorescence studies with eggPC SUV showed furthermore that an interaction between CF and vesicle membranes does exist which, however, involves only a few percent of the dye. The exact nature of this interaction is unclear but electrostatic effects are very likely. Such behavior would very well explain the differences in our quenching curves (Figure 2). The interaction of CF with DOPC− and POPC−SUV are presumed to be different because of the extreme curvature where membrane defects enhance the incorporation of dye molecules into the membrane and possibly lead to dissimilarities in the lipid order. Since the quenching curve is practically the same for all LUV systems, such differences are apparently negligible for the larger (less curved) vesicles. The possible mechanism of self-quenching can be assumed to be much faster than the pore formation. Therefore it does not affect our interpretation of the efflux data. The fluorescence change (described by the static Q_o) is simply exploited as a signal that monitors the extent of efflux in terms of our kinetic model which is probe-independent.

By virtue of analyzing the transient quenching factor Q_t over the course of an efflux experiment, we have determined a pertinent single-pore retention factor ρ indicating a graded efflux mode in each of our vesicle systems (Table 2). First of all we note that this quantity is not significantly altered by the lipid species involved. On the other hand, however, our data clearly suggest substantial differences between pores upon changes of the vesicle size. If, for instance, the pores in LUV_{200} had identical properties when formed in LUV_{100} and SUV we expect an increase of τ_p/τ_o by a factor of 13 and 3000, respectively, (because of the accordingly reduced internal volume). This would imply $\rho = 0.28$ for POPC−LUV_{100} (0.39 for DOPC), and $\rho = 0$ for the SUV, which is obviously inconsistent with our measured values. Consequently the pore quality regarding marker permeability and/or lifetime must be much better in the larger vesicles (so that a larger amount of effluent can be released through a single pore), particularly when the LUV_{100} are compared with the SUV.

As far as the pore formation kinetics is concerned, the situation is basically the same for all our vesicle systems. The various specific parameters are collected in Table 3. They are subject to an experimental uncertainty of ±(20−50)%. Therefore moderate differences between the individual vesicle systems must not be overrated.

For k_1 and k_2 we see that there is no significant influence of lipid composition or vesicle size. Generally, k_1 is always about a magnitude larger than k_2. The reduced rate amplitudes for POPC appear to be significantly higher than those for DOPC at a constant vesicle size. This confirms previous findings of a more enhanced efflux for POPC- than for DOPC-vesicles (Rex, 1996).

CONCLUSIONS

Our experiments demonstrate that even very small amounts of melittin, possibly less than one bound monomer per 10^4 lipid molecules, can cause leakage of CF out of vesicles. This clearly suggests peptide induced formation of pores (i.e., isolated leaky patches in the bilayer).

We definitely observe a mode of graded efflux. It can be quantitatively characterized by a single-pore retention factor, ρ, which is related to the pore lifetime. Our results show that the pores in larger vesicles are much more efficient (suggesting larger cross sections and/or longer lifetimes).

The originally registered dequenching signal of released dye over the course of time could be converted into the rate of pore openings per vesicle. This curve reflects a pronounced slowing down which can in any case be very well fitted by two exponential time functions with relaxation times at about 20 and 200 s, respectively. These relaxation times do not significantly change upon increasing the ratio of bound peptide per lipid. They also remain practically independent of the chosen liposome conditions. The rate amplitudes, however, increase in proportion to the concentration of bound melittin. In the POPC−LUV a larger rate of pore openings is induced than in the comparable DOPC case.

Because of the observed kinetic features we infer that two intermediate states of bound monomeric peptide are rate determining for the overall pore formation process. A basic scheme of relevant reaction steps has been proposed that indeed provides a quantitative reproduction of our experimental results.

ACKNOWLEDGMENT

We thank Dr. Ingrid Weis for her assistence in measuring the quenching curves and Christoph Stürzinger for performing the binding experiments. We are also very grateful to Dr. Frank Stieber (Institute of Physical Chemistry of this university) for making available to us the DLS measuring apparatus and giving expert advice in discussing our results.

APPENDIX

We may supplement a few relevant comments regarding the mathematical treatment of the proposed reaction Scheme 1. According to standard routines the rate equation fot the A_1-state reads

$$dr_1/dt = k_{01}r_0 - (k_{10} + k_{12})r_1 + k_{21}r_2$$

The variable r_0 can be eliminated by means of eq 3. Due to the fast partitioning between the A_{free}- and A_0-states we have $r_0/r = c_P'/c_P$ where $c_P' = c_P - c_L(r_1+r_2)$ stands for the concentration of peptide participating in this partitioning. Also we may neglect the final steady state values of r_1 and r_2. Then we obtain the relation $r_0 = r - x_{as}(r_1 + r_2)$. The quantity r is independent of time (being equal to the peptide to lipid ratio that can be derived from our binding experiments). Now we arrive at

$$dr_1/dt = k_{01}r - (k_{10} + k_{12} + x_{as}k_{01})r_1 + (k_{21} - x_{as}k_{01})r_2 \quad \text{(A1a)}$$

$$dr_2/dt = k_{12}r_1 - (k_{21} + k_{23})r_2 \quad \text{(A1b)}$$

These two linear differential equations for r_1 and r_2 can generally be solved under any conditions by means of well-known textbook procedures. The resulting time function for r_2 (to be inserted in eq 10) will actually feature two relaxation terms and a final steady-state value $\boldsymbol{r}_2$. Because of the condition 11 ($k_{01} \ll k_{12}$, k_{21}) the result can be much more simplified. Then the x_{as}-terms in eq A1a may be neglected. Also one can assume a steady state of the presumably faster step $A_1 \rightleftharpoons A_2$ in the slower time range (implying that dr_2/dt

$= 0$ holds there). In this way the r_2-term can be eliminated in eq A1a so that it turns into the simple form

$$dr_1/dt = -k_2(r_1 - \boldsymbol{r}_1) \quad \text{with} \quad k_2 = k_{10} + k_{12}k_{23}/(k_{21} + k_{23}), \quad \boldsymbol{r}_1 = (k_{01}/k_2)r \quad \text{(A2a)}$$

The solution of this differential equation is readily obtained as

$$r_1 = \boldsymbol{r}_1 + (r_{10} - \boldsymbol{r}_1)\exp(-k_2 t) \quad \text{(A2b)}$$

where r_{10} stands for the zero-time value of r_1 (i.e., the population of A_1 having been generated in the initial perturbation period). On the other hand, $\boldsymbol{r}_1$ denotes the finally established steady state value of r_1. By inserting eq A2b into eq A1b it follows

$$dr_2/dt + k_1 r_2 = k_{12}[\boldsymbol{r}_1 + (r_{10} - \boldsymbol{r}_1)\exp(-k_2 t)] \quad \text{where} \quad k_1 = k_{21} + k_{23} \gg k_2 \quad \text{(A3a)}$$

The general solution of eq A3a is now available as

$$r_2 = \boldsymbol{r}_2 + (k_{12}/k_1)(r_{10} - \boldsymbol{r}_1)\exp(-k_2 t) + [r_{20} - (k_{12}/k_1)r_{10})]\exp(-k_1 t), \; \boldsymbol{r}_2 = (k_{12}/k_1)\boldsymbol{r}_1 \quad \text{(A3b)}$$

With $r_2 = r_{20}$ at $t = 0$ (initial perturbation period) one may now apply eq 10 and then go on to the appropriate $v^* = v/rN_L$. Eventually this results in

$$v^* = v_1^* \exp(-k_1 t) + v_2^* \exp(-k_2 t) + v_3^*$$

where

$$v_1^* = k_{23}[x_{20} - (k_{12}/k_1)x_{10}], \quad v_2^* = k_{23}(k_{12}/k_1)[x_{10} - \boldsymbol{x}_1]; \quad v_3^* = k_{23}\boldsymbol{x}_2$$

In this context $x_{10} = r_{10}/r$, $x_{20} = r_{20}/r$, and $\boldsymbol{x}_1 = (k_{01}/k_2)$, $\boldsymbol{x}_2 = (k_{12}/k_1)\boldsymbol{x}_1$ stand for the mole fractions of bound peptide in the transient A_1, A_2-states at $t = 0$, and under the condition of the final steady state, respectively.

REFERENCES

Arbuzova, A. (1996) Ph.D. Thesis, University of Basel, Switzerland.
Arbuzova, A., & Schwarz, G. (1996) *Progr. Colloid Polym. Sci. 100*, 345−350.
Barbet, J., Machy, P., Truneh, A., & Leserman, L. D. (1984) *Biochim. Biophys. Acta 772*, 347−356.
Benachir, T., & Lafleur, M. (1995) *Biochim. Biophys. Acta 1235*, 452−460.
Böttcher, C. F. J., van Gent, C. M., & Fries, C. (1961) *Anal. Chim. Acta 24*, 203−204.
Chen, R. F. & Knutson, J. R. (1988) *Anal. Biochem. 172*, 61−77.
Dempsey, C. E. (1990) *Biochim. Biophys. Acta 1031*, 143−161.
Ellens, H., Bentz, J., & Szoka, F. C. (1984) *Biochemistry 23*, 1532−1538.
Fattal, E., Nir, S., Parente, R. A., & Szoka, F. C. (1994) *Biochemistry 33*, 6721−6731.
Grant, E., Beeler, T. J., Taylor, K. M. P., Gable, K., & Roseman, M. A. (1992) *Biochemistry 31*, 9912−9918.
Hellmann, N., & Schwarz, G. (1998) *Biochim. Biophys. Acta* (in press).
Hope, M. J., Bally, M. B., Mayer, L. D., Janoff, A. S., & Cullis, P. R. (1986) *Chem. Phys. Lipids 40*, 89−107.
Huang, C., & Mason, J. T. (1978) *Proc. Natl. Acad. Sci. U.S.A. 75*, 308−310.
Kuchinka, E., & Seelig, J. (1989) *Biochemistry 28*, 4216−4221.
Ladokhin, A. S., Wimley, W. C., & White, S. H. (1995) *Biophys. J. 69*, 1964−1971.
Ladokhin, A. S., Selsted, M. E., & White, S. H. (1997) *Biophys. J. 72*, 1792−1766.
Liu, Z.-Y., Solow, R., & Hu, V. W. (1988) *Biochim. Biophys. Acta 945*, 253−262.
Matsuzaki, K., Harada, M., Handa, T., Funakoshi, S., Fujii, N., Yajima, H., & Miyajima, K. (1989) *Biochim. Biophys. Acta 981*, 130−134.
Matsuzaki, K., Harada, M., Funakoshi, S., Fujii, N., & Miyajima, K. (1991) *Biochim. Biophys. Acta 1063*, 162−170.
Matsuzaki, K., Murase, O., Tokuda, H., Funakoshi, S., Fujii, N., & Miyajima, K. (1994) *Biochemistry 33*, 3342−3349.
Matsuzaki, K., Murase, O., Fujii, N., & Miyajima, K. (1995a) *Biochemistry 34*, 6521−6526.
Matsuzaki, K., Murase, O., & Miyajima, K. (1995b) *Biochemistry 34*, 12553−12559.
Mayer, L. D., Hope, M. J., & Cullis, P. R. (1986) *Biochim. Biophys. Acta 858*, 161−168.
Ostolaza, H., Bartolomé, B., Ortiz de Zaraté, I., De la Cruz, F., & Goñi, F. M. (1993) *Biochim. Biophys. Acta 1147*, 81−88.
Parente, R., Nir, S., & Szoka, F. C. (1990) *Biochemistry 29*, 8720−8728.
Quay, S. C., & Condie, C. C. (1983) *Biochemistry 22*, 695−700.
Rapaport, D., & Shai, Y. (1991) *J. Biol. Chem 266*, 23769−23775.
Rapaport, D., Peled, R., Nir, S., & Shai, Y. (1996) *Biophys. J. 70*, 2502−2512.
Rex, S. (1995) Ph.D. Thesis, University of Basel, Switzerland.
Rex, S. (1996) *Biophys. Chem. 58*, 75−85.
Sansom, M. S. P. (1991) *Prog. Biophys. Mol. Biol. 55*, 139−235.
Schwarz, G., Gerke, H., Rizzo, V., & Stankowski, S. (1987) *Biophys J. 52*, 685−692.
Schwarz, G., & Beschiaschvili, G. (1989) *Biochim. Biophys. Acta 979*, 82−90.
Schwarz, G., & Robert, C. H. (1990) *Biophys. J. 58*, 577−583.
Schwarz, G., & Robert, C. H. (1992) *Biophys. Chem. 42*, 291−296.
Schwarz, G., Zong, R., & Popescu, T. (1992) *Biochim. Biophys. Acta 1110*, 97−104.
Schwarz, G., & Arbuzova, A. (1995) *Biochim. Biophys. Acta 1239*, 51−57.
Schwarz, G. (1996) *Biophys. Chem. 58*, 67−73.
Sekharam, K. M., Bradrick, T. D., & Georghiou, S. (1991) *Biochim. Biophys. Acta 1063*, 171−174.
Shai, Y., Bach, D., & Yanofsky, A. (1990) *J. Biol. Chem. 265*, 20202−20209.
Shai, Y., Hadari, Y. R., & Finkels, A. (1991) *J. Biol. Chem. 266*, 22346−22354
Weinstein, J. N., Yoshikami, S., Henkart, P. Blumenthal, R., & Hagins, W. A. (1977) *Science 195*, 489−492.
Weinstein, J. N., Klausner, R. D., Innerarity, T., Ralston, E., & Blumenthal, R. (1981) *Biochim. Biophys. Acta 647*, 270−284.
Yanni, Y. P., Fitton, J. E., & Morgan, C. G. (1986) *Biochim. Biophys. Acta 856*, 91−100.

BI971009P